JMEPEG (2020) 29:1068–1079
https://doi.org/10.1007/s11665-020-04617-z

1059-9495/$19.00

Effects of Filler Metals on Heat-Affected Zone Cracking in IN-939 Superalloy Gas-Tungsten-Arc Welds

H. Kazempour-Liasi, M. Tajally, and H. Abdollah-Pour

(Submitted September 7, 2019; in revised form January 4, 2020; published online February 5, 2020)

Filler metals play an important role in reducing the weld cracking in nickel-based superalloys. In order to improve the welding conditions of IN939 superalloy, a wide range of solid solutions and age-hardenable filler metals were investigated in this study. Five solid solutions (HAYNES 230, IN625, IN617, HASTELLOY X, HAYNES 25) and two precipitation-strengthened alloys (IN718, HAYNES C-263) were used as filler metal to weld IN939 superalloy via gas-tungsten-arc welding. Microstructural studies were performed using optical microscopy and field-emission scanning electron microscopy. The results revealed that IN939 alloy is susceptible to liquation cracking in the heat-affected zone. In addition, the primary γ′ particles had grown into "ogdoadically diced cubes" of about of 2 µm in side length. The microstructure of the weld pool made with various filler metals was observed to be made up of fine spherical γ′ particles with a diameter of about 0.2 µm. The study of mechanical properties and thermodynamic behavior of the weld showed that the filler metals with lower concentrations of (Al + Ti + Nb + Ta + Mo + W) than the base metal can effectively attenuate the PWHT cracking. We found that optimal IN939 alloy weld performance can be achieved using HAYNES C-263 as filler metal, followed by IN617 and then IN625.

Keywords IN939, TIG, weld, filler metal, HAZ, liquation cracking

1. Introduction

Tungsten inert gas (TIG) welding has been used for joining particular materials such as Ni alloy for high-quality welding (Ref 1). In addition, this process has been widely used to repair gas turbine and engine components (Ref 2, 3). Precipitation-strengthened Ni-based superalloys have been widely used in the manufacturing of hot gas path components for aircraft and industrial gas turbines, where the component is designed for high-stress and high-temperature operating conditions. Fusion welding has been the process of choice for joining and repairing such components. However, weldability of superalloys containing high Ti and Al contents, which are known to form γ′ precipitate, is poor due to their high susceptibility to heat-affected zone (HAZ) cracking (Ref 4). As a Ni-based superalloy, IN939 is hardened by precipitation of the γ′ phase. This alloy was first designed for use in the blades of gas turbines (Ref 5, 6).

Chemical composition of the base metal, microstructure of the weld, welding parameters and pre- and post-weld heat treatments can affect the HAZ cracking (Ref 4-8). Composition of the filler metal is also an important factor affecting the extent of liquation cracking in the HAZ. Investigations on IN738LC have shown that an increase in the Al concentration of the filler metal can add to the chance of cracking. Indeed, this element increases the volume fraction of the γ′ phase and hardness of the weld pool, thereby restraining plastic deformation of the weld pool. Moreover, reduced ductility of the weld pool tends to transmit the stresses induced upon the welding process to the HAZ in the form of tensile stress, causing crack formation in this zone (Ref 9). The optimum contents of Al, Ti and C in IN738 filler metal were reportedly 3, 2 and 0.26%, respectively (Ref 10). The presence of other elements such as Ti, Nb and Ta in the composition of filler metal can, by creating secondary phases such as MC carbides, not only increase the hardness of the weld pool region, but also affect the tendency of HAZ to constitutional liquation (Ref 11). In addition to the concentration of (Al + Ti), the use of filler metals with a small γ-γ′ mismatch tends to harden the resultant weld and slower the response to the aging process, thereby reducing the HAZ cracking (Ref 12). Generally, solid-solution filler metals, such as IN625, represent the alternative of choice for reducing the cracking during welding of precipitation-strengthened superalloys. However, the need for welding in the high-stress zones of parts or for repairing the parts used in high-temperature operating conditions restricts the use of the solid-solution filler metals as those cannot be strengthened via heat treatment, in which case one needs age-hardenable filler metals (Ref 12). With a lower (Al + Ti) concentration than that of the base metal, the age-hardenable filler metals can be effective in reducing the strain-age cracking (SAC) during post-weld heat treatment (PWHT) (Ref 13). In addition to the filler metal composition, its properties and cost are also important factors (Ref 14, 15).

The effect of the filler metal on HAZ cracking of some nickel-based alloys, such as IN738 (Ref 9-14), has been previously investigated. However, the effect of the filler metal on HAZ cracking of IN939 is yet to be reported. In this work, effects of pre-weld heat treatment and various filler metals (HAYNES 230, IN625, IN617, IN718, HASTELLOY X,

H. Kazempour-Liasi, Faculty of Materials and Metallurgical Engineering, Semnan University, Semnan, Iran; and Metallurgy Department, Niroo Research Institute, Tehran 14686, Iran; and **M. Tajally** and **H. Abdollah-Pour**, Faculty of Materials and Metallurgical Engineering, Semnan University, Semnan, Iran. Contact e-mail: m_tajally@semnan.ac.ir.

HAYNES 25 and HAYNES C-263) on microstructure and HAZ cracking of TIG-welded IN939 were examined. For this purpose, solid-solution (HAYNES 230, IN625, IN617, HASTELLOY X, HAYNES 25) and precipitation-strengthened (IN718, HAYNES C-263) filler metals were used.

2. Materials and Methods

Coupons with dimensions of 2 × 2 × 8 cm were cut from IN939-made gas turbine blades using a wire electrical discharge machine (WEDM). Table 1 presents the chemical composition of the IN939. A total of seven coupons were prepared for welding with seven filler metals (Fig. 1).

Experiments were performed in two steps. In the first step, in order to investigate liquation cracking, the coupons were subjected to pre-weld heat treatment. In the next step, the weld region was investigated for strain-age cracking during the PWHT. For this purpose, the welded coupons were subjected to standard four-stage PWHTs (as detailed in Table 2) followed by examining the cross section of the samples.

In this study, we used IN625, IN617, IN718, HAYNES 230, HAYNES 25, HASTELLOY X and HAYNES C-263 as filler metals, which were solid-solution alloys, except for IN718 which was a precipitation-strengthened alloy. All of the studied filler metals were nickel-based superalloys, while the HAYNES 25 was based on cobalt. Chemical compositions of these filler metals are reported in Table 3. Welds were performed via TIG welding using a filler metal wire of 1.2 mm in diameter and 160-A, 10-V electric current.

The welded coupons were sectioned transversely to the welding direction using the WEDM. Next, the cross section of the coupons was polished, etched and then examined for investigating the susceptibility of the welds to cracking by measuring the total crack length (TCL) per section. The specimens were etched in a solution containing 0.3 g of MoO_3, 10 ml of HNO_3, 10 ml of HCl and 15 ml of H_2O. Optical microscopy (OM) was used to measure the crack length on the samples. Prior to the microstructural study, the samples were ground down to 0.5 mm to remove possible results of oxidation and depleted layers. Microstructural characteristics were studied via OM and field-emission scanning electron microscopy (FESEM) on a TESCAN-MIRA3, while chemical compositions of the secondary phases were examined through energy-dispersive x-ray spectroscopy (EDS). In order to investigate the relationship between the hardness of the filler metal and crack formation in the weld region, the Vickers hardness method was used. The mechanical properties of the weldments were also examined by tensile testing at room temperature according to ASTM E8 standard test procedure. Elemental distribution and thermodynamic analyses were performed using the JMatPro software package coupled with the Ni-DATA database.

3. Results and Discussion

3.1 Liquation Cracking in the HAZ

The OM micrographs of the HAZ in the samples welded with different filler metals are shown in Fig. 2. According to this figure, the HAZ cracking was evident for the samples welded with IN718, HAYNES 25, H230 and HASTELLOY X. However, the pre-weld heat-treated samples welded with the C263 filler metal showed no evidence of HAZ cracking. The microstructure of the as-received IN939 consisted of primary (MC) and secondary carbides ($M_{23}C_6$) and primary and secondary γ' particles with a fineness of 20 to 150 nm. In this condition, the hardness of the base alloy was about 470 HV. In order to reduce the hardness to enhance the weldability of the specimens (Ref 16, 17), samples were subjected to pre-weld heat treatment. Consequently, the hardness of pre-weld heat-treated samples was decreased to about 310 HV. Figure 3 shows OM and FESEM images of the γ' particles in the pre-weld heat-treated samples. In terms of microstructure, the samples were composed of primary MC carbides, very coarse primary γ' particles with dimensions of about 1 to 2 microns and γ-γ' eutectic phases (Fig. 3a). Accordingly, liquation cracking was expected due to the presence of eutectic microstructures and coarse γ' particles. Pre-weld heat-treated samples exhibited evidence of η phases in their microstructure, which could be attributed to HAZ cracking via the constitutional liquation mechanism (Ref 15). According to Fig. 3(b), the primary γ' particles were grown into 1-2 μm-sided cubes and "ogdoadically diced cubes," while the secondary γ' particles were completely solved in the matrix with no chance of nucleation and growth given that this type of γ' particles

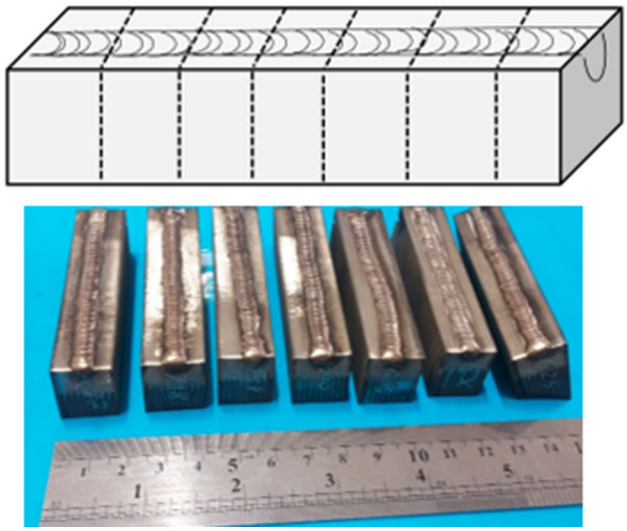

Fig. 1 The coupons prepared via the bead-weld configuration in this work

Table 1 Chemical composition of the base alloy (IN939) (Ref 5, 6)

Element	Al	Ti	B	W	Ta	Cr	C	Fe	Nb	Si	Mn	Zr	Co	Ni
wt.%	2.0	3.7	0.014	2.2	1.4	22.5	0.15	0.5	1.1	0.2	0.2	0.14	19	Bal.

Table 2 Pre- and post-weld heat treatment cycles applied in this work

Heat treatments	Description
Pre-weld heat treatment	1160 °C/4 h/FC/to 920 °C(rate 0.5 °C/min)/AC
Post-weld heat treatment	1160 °C/4 h/AC + 1000 °C/6 h/FAC + 900 °C/24 h/AC + 700 °C/16 h/AC

FAC fast air cool, *AC* air cool, *FC* furnace cool

Table 3 Chemical compositions of the filler metals used in this study (wt.%) (Ref 9, 14, 15)

Trade name of filler metal	Cr	Ni	Co	Mo	W	Nb	Ti	Al	Fe	C	Other	Strengthening mechanisms
HAYNES® 230-W	22	Bal.	5	2	14	…	…	0.35	3	0.1	0.5 Si, 0.6 Mn	SSS
INCONEL® 625	21.5	Bal.	…	9		3.6	0.4	0.4	5	0.1	0.5 Mn, 0.5 Si	SSS
INCONEL® 617	22	Bal.	12.5	9	…	…	…	1	3	0.07	1 Mn, 1 Si	SSS
INCONEL®718	19	Bal.	…	3	…	5.1	0.9	0.5	18.5	0.08	0.15 Cu	PS
HASTELLOY®X RTW™	22	Bal.	1.5	9	0.6	…	…	2	18	0.15	…	SSS
HAYNES®25 RTW™	20	10	Bal.	…	15	…	…	…	3	0.1	1.5 Mn	SSS
HAYNES®C-263 RTW™	20	Bal.	20	5.9	…	…	2.1	0.45	0.7	0.06	…	PS

SSS solid-solution-strengthened, *PS* precipitation-strengthened

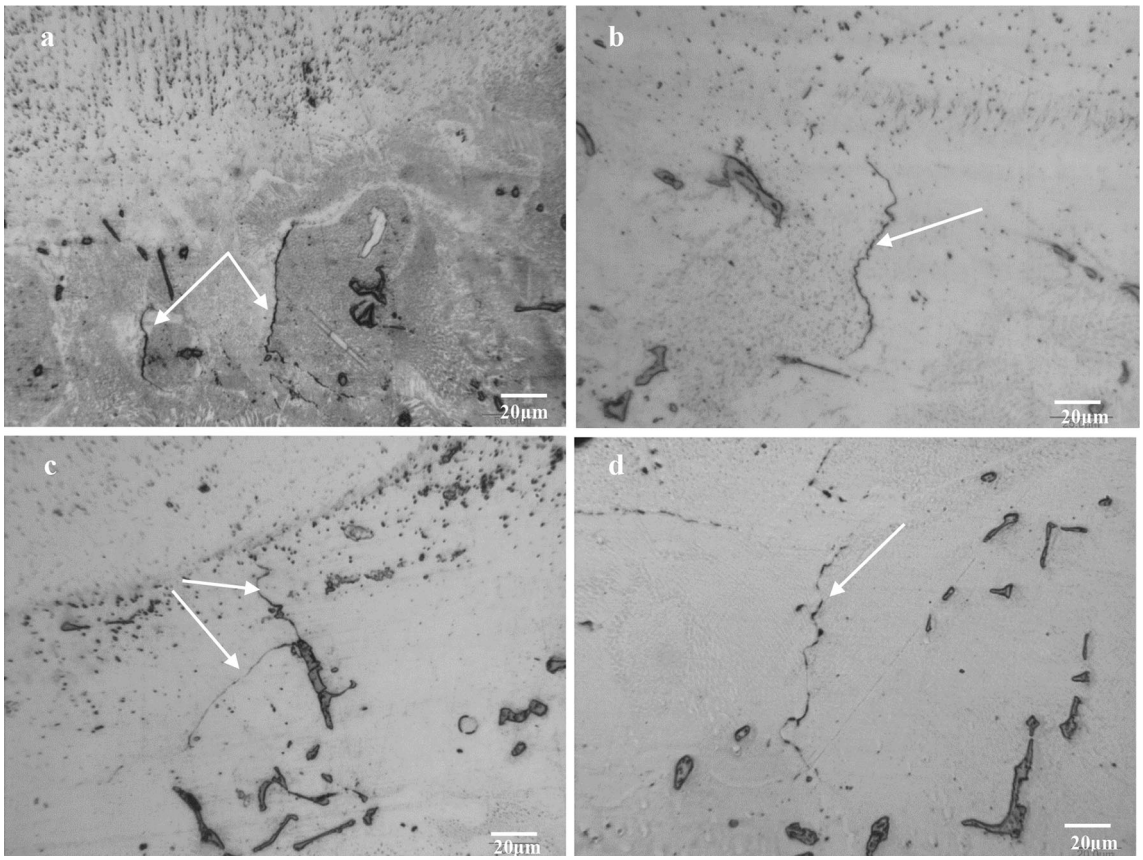

Fig. 2 The OM micrograph of HAZ cracking on the samples welded with different filler metals: (a) HASTELLOY X, (b) HAYNES 230, (c) HAYNES 25 and (d) IN718. Cracks are marked with arrows

form upon coarsening of coherent γ′ particles. The driving force behind this particle development is to minimize the misfit energy and the interface energy between γ and γ′ phases. In this case, the cubic primary γ′ particles had grown from the corners (Ref 18, 19).

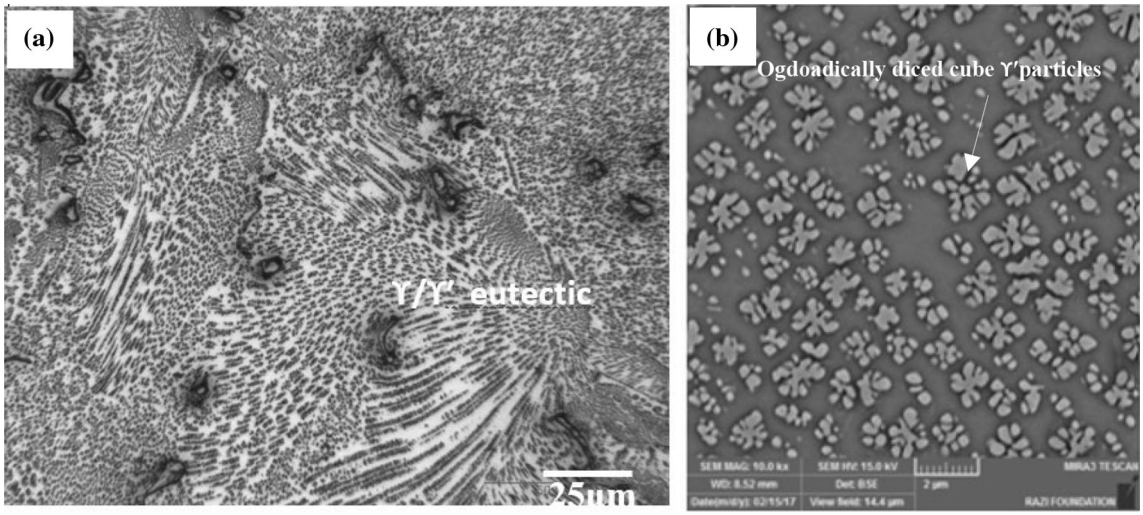

Fig. 3 (a) The OM and (b) FESEM micrographs of the γ′ particles and eutectic phases in the pre-weld heat-treated base metal

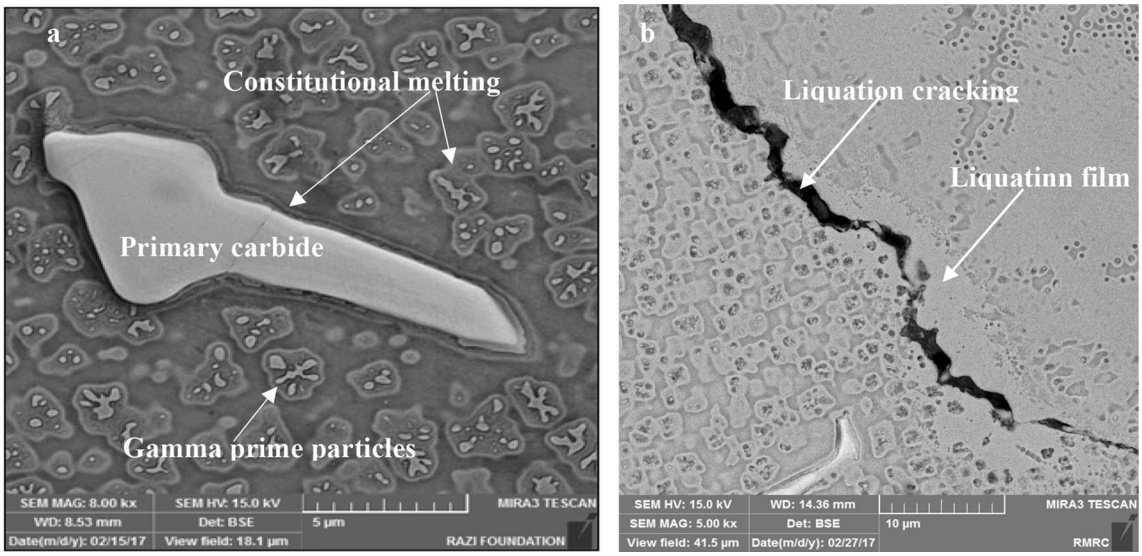

Fig. 4 FESEM image of (a) constitutional melting of the carbide and γ′ particles, and (b) liquation cracking in the HAZ

Figure 4 shows the FESEM image of a primary carbide and γ′ particles in the HAZ. The presence of a melting area in this figure confirms that carbide and γ′ particles were melted during the welding process (Fig. 4a). Dissolution rates of the secondary phases are known to be functions of the shape and size of the precipitate (Ref 17, 20). Given that the dissolution kinetics of larger precipitates is slower than that of the smaller ones (Ref 17), during the welding process, the γ′ particles are expected to be solved faster than the carbide particles (see Fig. 4a). Therefore, the contribution of the γ′ particles to the formation of liquid films (Fig. 4b) in the HAZ is larger than that of the carbide particles.

The melting phenomenon around the weld and the diffusion of the liquid phase through the grain boundaries or between the phases and the matrix would cause liquation cracking in the HAZ (Ref 5). In other words, upon intergranular liquation, the non-equilibrium liquation of secondary phases (e.g., γ′ particles, MC-carbide and γ-γ′ eutectic phases) existing in the pre-weld base material leads to crack formation (Ref 17).

Figure 5 demonstrates the measurement results in terms of the total number of cracks (TNC) and total crack length (TCL) on pre-weld heat-treated samples as well as the samples welded with various filler metals. According to this figure, HAYNES C-263 followed by IN617 and IN625 was found to be the best filler metals for minimizing crack formation around the weld area in IN939 alloy. The figure further shows various amounts of crack in different specimens in terms of the filler metal used for welding, because of differences in physical and mechanical properties of the filler metals. Indeed, the results highlighted higher susceptibility to cracking for the welds made with the filler metals of higher hardness and strength. More generally, the higher the welding stresses, the higher will be the chance of liquation crack formation around the weld.

3.2 Hardness of Weld Pools

Figure 6 shows the measured hardness of the samples prior to and after PWHT. According to the results, the PWHT sample welded using HAYNES C-263 as filler metal exhibited the

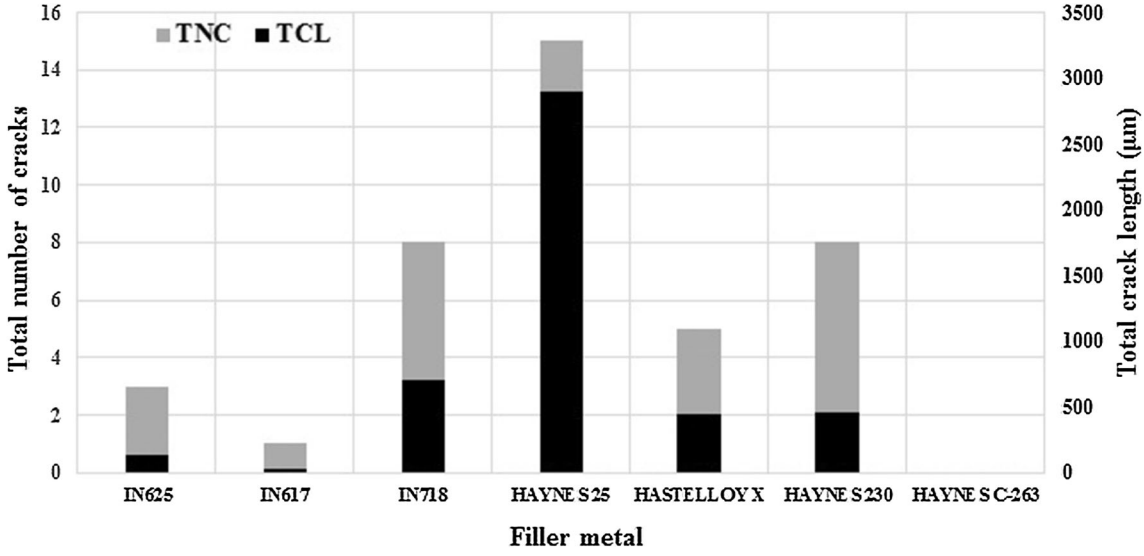

Fig. 5 Results of the crack formation studies on cross sections of the pre-weld heat-treated specimens welded with different filler metals

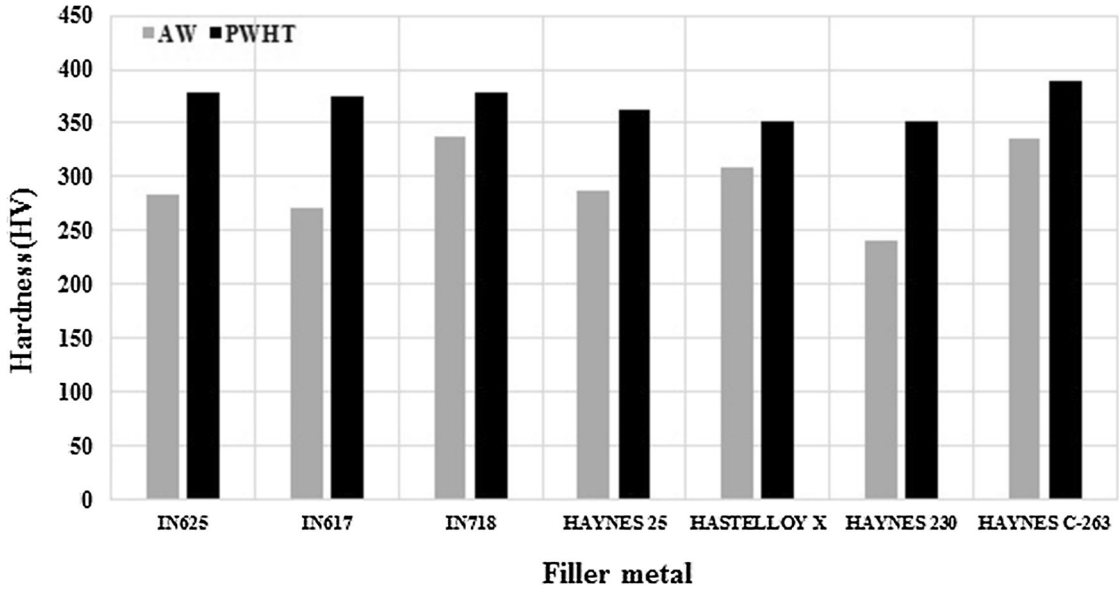

Fig. 6 Results of hardness value of weld pool, as-weld (AW) and PWHT condition (HV)

highest hardness, with the strength of the weldment being much closer to that of the base metal (IN939). Therefore, considering the resultant mechanical properties and crack formation, HAYNES C-263 filler metal was found to be the optimal metal for welding IN939 superalloy.

Comparing the as-weld samples with those subjected to PWHT, one can see the significant increase in hardness upon the PWHT. However, given that most of the filler metals studied in this study were solid solutions (which are expected not to change their hardness upon heat treatment), the increased hardness could be attributed to changes in the chemical composition of the weld pool due to dilution of the filler and base metal during the welding process. Table 4 presents the dilution (D) and chemical composition of the weld pools for various filler metals. During the welding process, the aluminum and titanium elements (γ' formers) are added to the weld pool from the base metal, and subsequent formation of the γ' particles during the PWHT process increases the hardness of the weld pool.

3.3 Chemical Composition and Microstructure of Weld Pools

The formation of γ' particles in the weld pool was investigated by FESEM. Figure 7 shows images of the γ' particles ($\sim$ 0.2 μm) in the weld pools. The figure indicates that, in the corresponding weld pool to most of the studied specimens, the γ' particles were formed after the PWHT. Moreover, the highest amounts of the γ' phase were observed on the weld pools obtained using IN718 and C263 as filler metal, while IN625 and HAYNES25 returned the lowest. As mentioned earlier, this was due to the introduction of alloying elements (e.g., Al and Ti, as γ'-forming elements) from the base metal to the weld pool during the welding process (Table 4). It

Table 4 Dilution level (D) and chemical composition of the studied weld pools (wt.%)

Filler metal	D%	Cr	Ni	Co	Mo	W	Nb	Ti	Al	Fe	Ta	Al + Ti
IN625	57	22.07	52.96	11.26	3.87	1.25	2.2	2.28	1.31	2.44	0.86	3.59
IN617	60	22.7	50.14	16.4	3.6	1.32	0.66	2.46	1.6	1.5	0.584	4.06
IN718	65	22.28	48.86	12.7	1.05	1.43	2.5	2.72	1.48	5.86	0.91	4.2
HASTELLOY X	63	22.32	47.68	12.53	3.33	1.61	0.69	2.33	2.00	6.98	0.88	4.33
HAYNES 230	66	22.33	49.65	14.24	0.68	6.21	0.90	2.48	1.42	1.35	0.92	3.9
HAYNES 25	64	21.40	33.52	29.66	0.35	6.66	0.70	2.37	1.28	1.37	0.90	3.65
HAYNES C-263	63	21.58	48.42	19.37	2.18	1.39	0.69	3.11	1.48	0.57	0.88	4.59

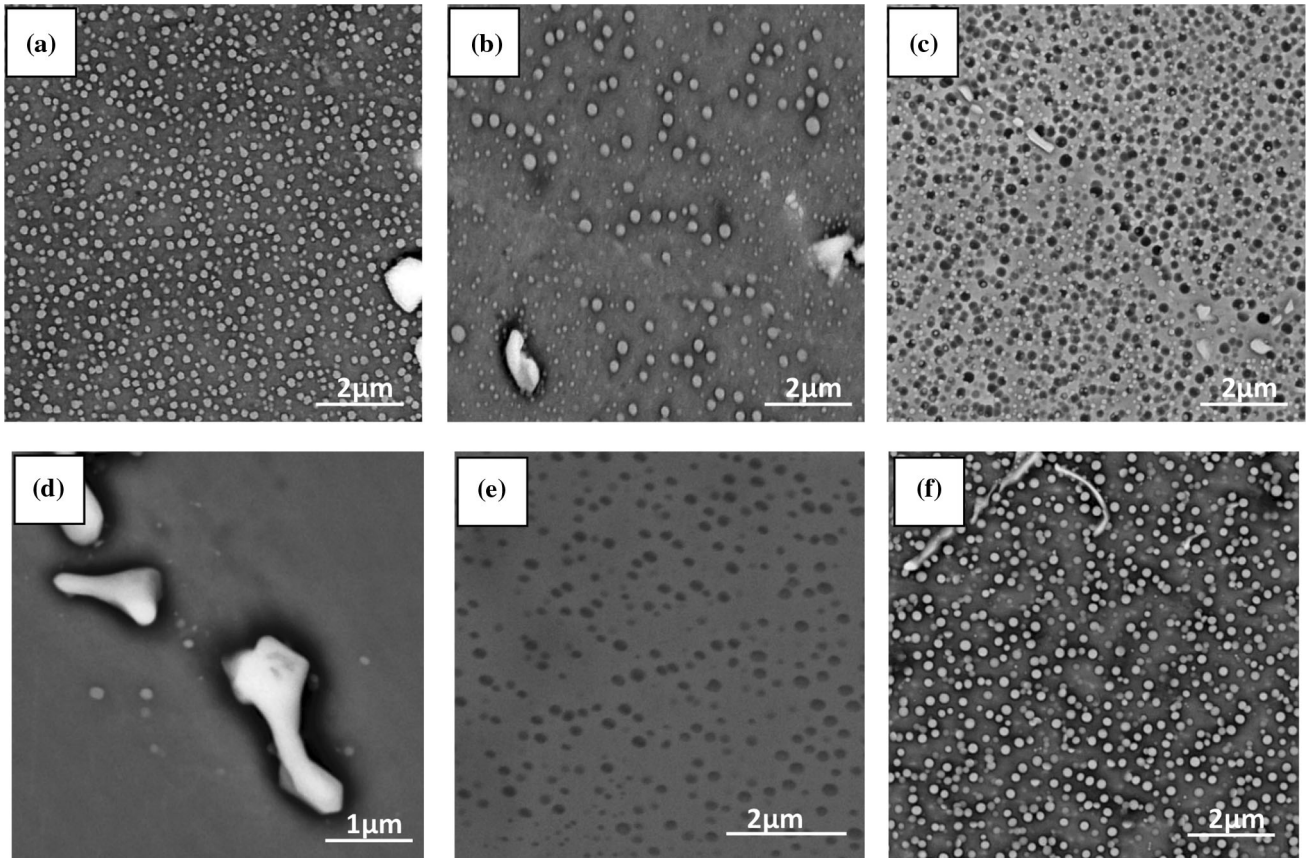

Fig. 7 FESEM micrographs indicating the formation of the γ′ particles, upon the PWHT, in the weld pools produced with (a) IN718, (b) IN617, (c) HAYNES C-263, (d) HAYNES 25, (e) IN625 and (f) HAYNES 230 as filler metal

is also clear from Fig. 8d that the carbide particles in the weld pool of HAYNES 25 (as filler metal) are much coarser and the percentage of the γ′ particles is significantly lower than those obtained by other filler metals. This could be due to the higher amount of carbide-forming elements (e.g., W) and the lower amount of the γ′-forming elements (Al, Ti) in the composition of this filler metal as well as the weld pool.

To confirm the presence of alloying elements in the weld pool, chemical investigations were performed using EDX analysis (Table 5). According to the results, the contents of Al and Ti in the weld pool were significantly higher than those in the original composition of the filler metals. These findings were well consistent with the calculated dilution level and microstructural studies (Table 4, Fig. 7).

In addition to Al and Ti, other elements were also found to be altered in the weld pool, with the extent of alteration depending on the type of filler metal (Fig. 8). Figure 9 presents plots of the total contents of Al, Ti, Nb, Ta and Mo as well as TCL for different filler metals. According to this figure, the highest contents of the elements were observed on the weld pool produced with HAYNES 25 as filler metal, while C263 produced the lowest contents when used as filler metal. This correlated well with the observed changes in cracks formation. Regarding the role played by these elements in the formation of secondary phases such as γ′ and carbides, one may refer to their effect on the liquation cracking upon constitutional melting of the secondary phases (carbide and γ′ particles) (Ref 17).

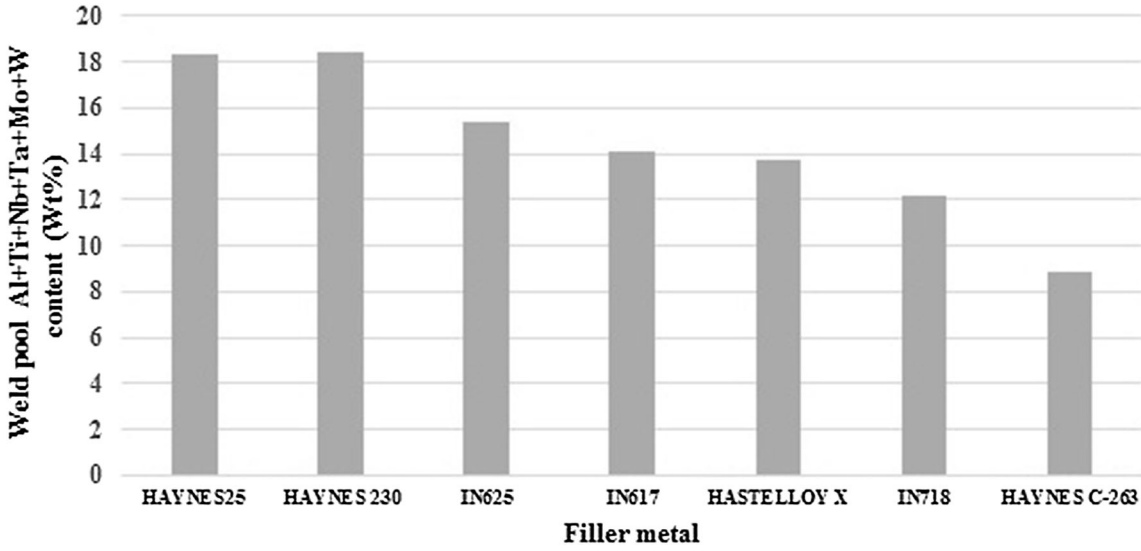

Fig. 8 Total contents of the Al, Ti, Nb, Ta, Mo and W in the weld pool for different filler metals

Table 5 EDX-measured chemical compositions of the studied weld pools (wt.%)

Filler metal	Cr	Ni	Co	Mo	W	Nb	Ti	Al	Fe	Other	Al + Ti
HAYNES 230	22.04	47.69	11.31	1.49	9.21	0.88	2.71	1.62	0.57	2.49 Ta	4.33
IN625	22.03	51	11.1	4.83	…	2.62	2.9	1.62	0.48	3.42 Ta	4.52
IN617	22.55	47.6	15.26	5	1.05	1.28	2.77	1.93	0.51	2.03 Ta	4.7
IN718	21.69	48.07	12.92	1.63	1.82	2.49	3.43	1.73	5.17	1.03 Ta	5.16
HASTELLOY X	22.36	45.18	12.34	4.82	1.12	1.05	2.73	1.56	6.42	2.41 Ta	4.29
HAYNES25	20.38	25.19	34.55	0.63	15.67	0.19	1.43	0.44	1.53	0	1.87
HAYNES C-263	20.52	50.06	18.71	3.93	0	0.62	3.24	1.07	0	1.84	4.31

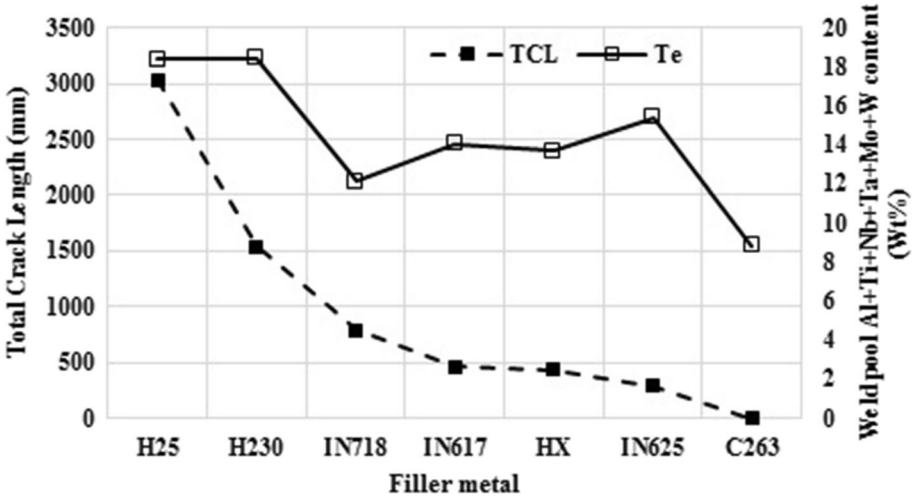

Fig. 9 Variations of the TCL and total contents of the key elements (Te) in the weld pool for different filler metals

3.4 Tensile Strength of Weldments

In order to select the optimal filler metal, mechanical properties of the weldments were examined through tensile testing at room temperature (Table 6). According to Table 6, it is clear that none of the specimens underwent failure within the weld area, and almost all of the specimens experienced failure within the base metal. Therefore, one may infer that no crack was formed in the weld area after the welding operation. This is consistent with the results of the microstructural studies indicating no crack in the weld area after the welding operation on the annealed samples. Therefore, it can be concluded that the annealing lowers the probability of liquation crack formation in IN939 alloy significantly.

Table 6 Measured mechanical properties of the specimens. The tests were performed at room temperature on both as-weld and PWHT-applied specimens

Filler metal	Condition	UTS, MPa	Elongation, %	Breakdown location
IN625	As weld	945 ± 6.94	10	Base metal
	PWHT	759 ± 6.73	5 ± 3.33	HAZ
IN617	As weld	1013 ± 10.54	13.33 ± 1.67	Base metal
	PWHT	754 ± 73	5 ± 1.67	HAZ
HAYNES C-263	As weld	897 ± 60	10.56 ± 3.5	Base metal
	PWHT	712 ± 10.84	4.44 ± 1.98	Base metal
HAYNES 230	As weld	817	…	Base metal
	PWHT	751 ± 13.34	6.11 ± 9.99	Base metal

According to the results of the tensile testing after PWHT, it is clear that the specimens welded with IN625 and IN617 (as filler metal) exhibited failure in the HAZ, while other specimens just broke out of the weld areas. This implies that the PWHT increases the susceptibility of the weld area to strain-age cracking. This confirms the results of the microscopic studies discussed in the previous sections. None of the specimens welded with HAYNES C-263 and HAYNES 230 as filler metal exhibited crack formation in the weld areas. Comparing the tensile strength of IN939 alloy upon the four-stage standard heat treatment with the results presented in Table 6, it can be concluded that the tensile strength of the weldment has been about 80% of that of the base metal.

3.5 Development of Appropriate Filler Metal for IN939 for Industrial Applications

3.5.1 Investigation of γ/γ′ Lattice Mismatch. Lattice mismatch is known to influence the strength of nickel-based alloys (Ref 21). The γ/γ′ mismatch affects the strain-age cracking during the PWHT (Ref 22). The unconstrained lattice mismatch (δ) is given by $\delta = 2(a_{\gamma'} - a_{\gamma})/a_{\gamma'} - a_{\gamma}$, where $a_{\gamma'}$ and a_{γ} are the lattice parameters of the γ′ and γ phases, respectively (Ref 21). The lattice mismatch may change with the morphology of the γ′ particles (Ref 22) and the temperature (Ref 21). Figure 10 presents simulated variations of the γ and γ′ lattice parameters with temperature (from room temperature up to 1100 °C) in the weld pool for different filler metals, as generated by the JMatpro software. According to Fig. 10, when either of HAYNES C-263 was used as filler metal, variations of the γ and γ′ lattice parameters with temperature resembled those of the base metal (IN939). On the other hand, with HASTELLOY X used as filler metal, changes in the γ and γ′ lattice parameters well differed from that of the base metal. Variation of the γ/γ′ lattice mismatch with temperature across the weld pool is presented in Fig. 11. According to this figure, the lattice mismatch remained relatively constant up to approximately 600 °C and then sharply reduced with temperature. This was because of the lower expansion coefficient of the γ′ phase, as compared to the γ phase (Ref 21). Given that the lattice mismatch provides a measure of the strain energy stored at the interface between γ and γ′ phases (Ref 21), a filler metal producing a closer lattice mismatch to the base metal is expected to be associated with lower strain in the weld pool (i.e., less susceptible to cracking). Variations of the γ and γ′ lattice parameters in the weld produced with HAYNES C-263 as filler metal were more similar to the γ′ lattice parameter in the base metal (IN939); this could lead to a reduction in the γ/γ′ lattice mismatch (Fig. 11) and hence strain in the HAZ. On the other hand, the γ/γ′ lattice mismatch was the largest with HASTELLOY X as filler metal, as compared to the other filler metals studied in this research (Fig. 11). These results are in agreement with the findings of metallographic studies and the TCL results.

Variations of the coefficient of thermal expansion (CTE) with temperature for different filler metals are shown in Fig. 12. The CTE difference between the base and filler metals can generate thermal stresses during the PWHT, leading to cracking of the welds (Ref 11). In this respect, the C263 had the closest CTE to that of the base metal (IN939), making it the filler metal of choice to minimize cracking of the weld.

3.5.2 Effect of Volumetric Changes Induced by the γ′ Precipitation. The linear dimension of precipitation-strengthened Ni-based superalloys is known to be directly proportional to the volume fraction of the γ′ phase precipitated from the solid-solution matrix during the aging treatments. Moreover, the volumetric changes resulted from the γ′ precipitation are known to affect the HAZ cracking during the PWHT (Ref 11). In this study, different values of γ/γ′ lattice mismatch were obtained with different filler metals (Fig. 11) because of the corresponding volumetric changes during the precipitation of the γ′ particles in the weld (see Fig. 13). These volumetric changes are given as:

$$\Delta v = \frac{(v_{\gamma'} - v_{\gamma})}{v_{\gamma}} \quad \text{(Eq 1)}$$

where $v_{\gamma'}$ and v_{γ} are the volumes of unit cells of γ and γ′, respectively. According to Fig. 13, the γ′ precipitation-induced volumetric changes of the specimen prepared with C263 as filler metal was closest to those of the base metal (IN939), leading to minimum stress and hence cracking in the HAZ.

3.5.3 Susceptibility of the Filler Metals to Solidification Cracking. As a metallurgical parameter, solidification temperature range (STR) is known to affect the susceptibility to solidification cracking (Ref 14). Differences in the chemical composition of the weld pools produced with different filler metals lead to corresponding differences in the STR. In the Nb-containing superalloys, a narrower STR indicates lower susceptibility to solidification cracking (Ref 14, 15, 23). Figure 14 reports the corresponding STR to the weld pools produced with different filler metals. According to Fig. 14, the results of JMatpro software are well correlated to the corresponding experimental data. The presence of Nb in chromium-rich

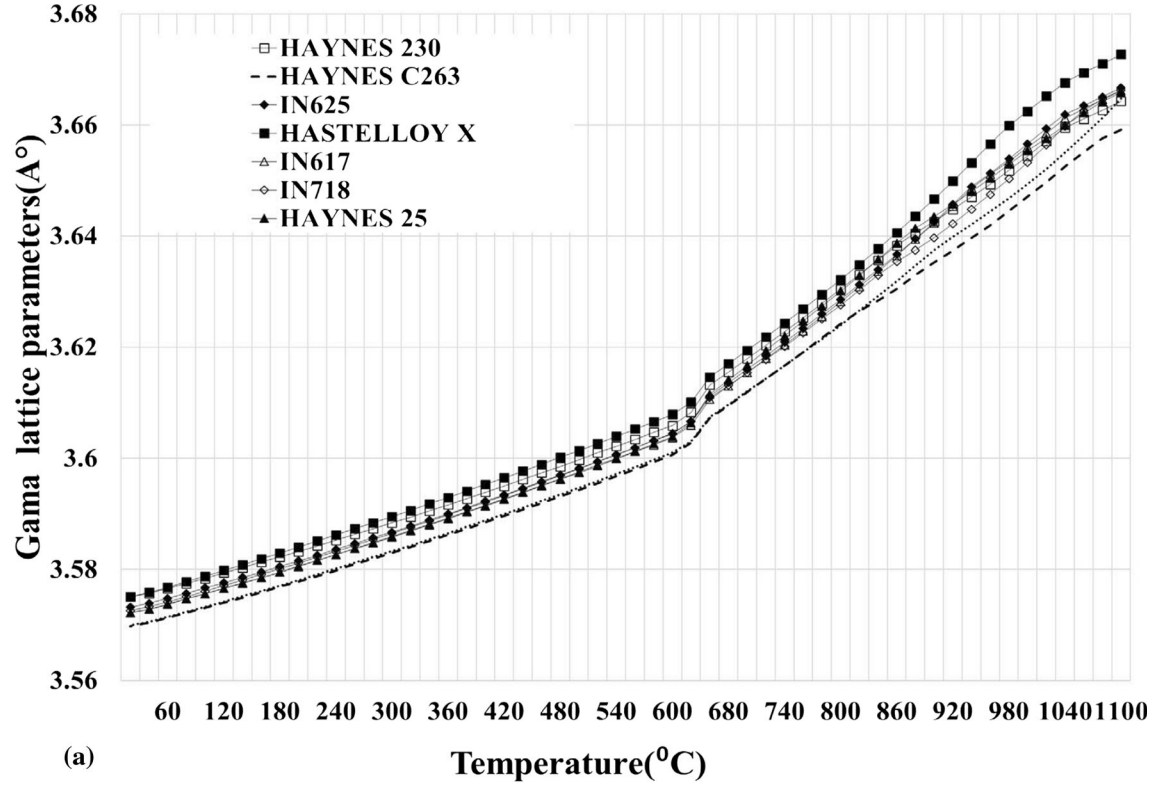

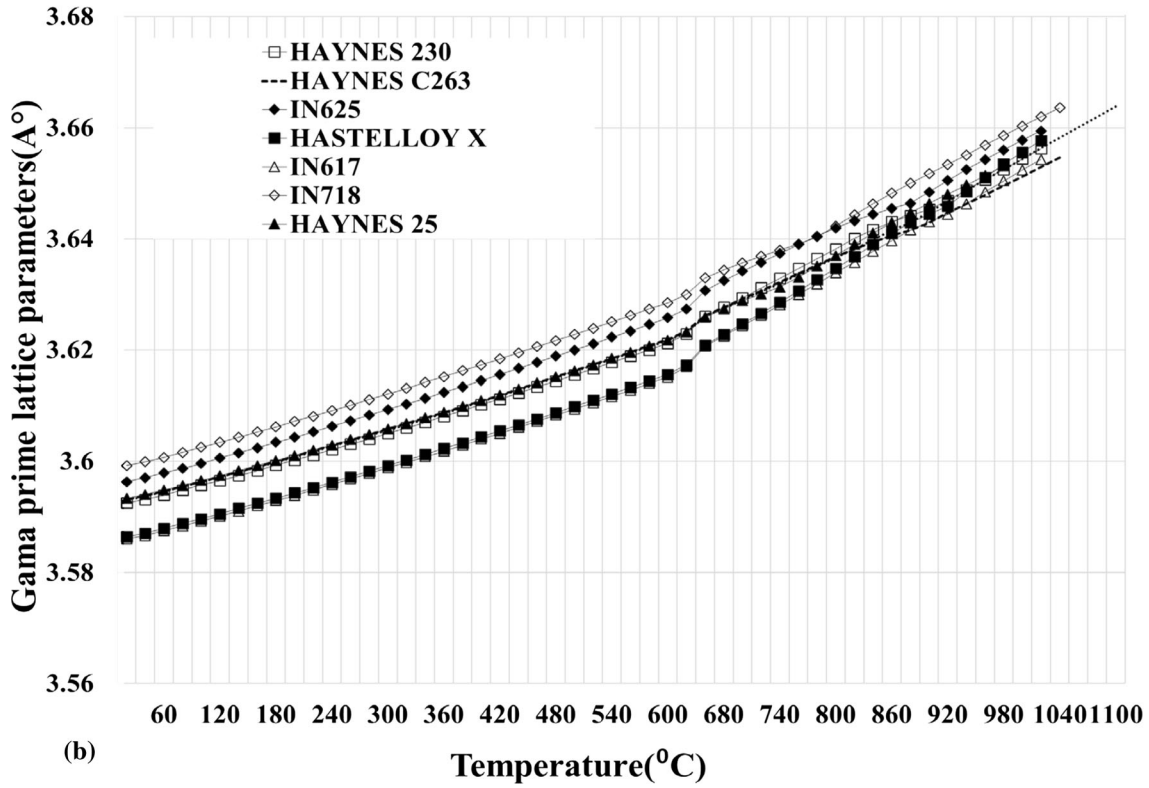

Fig. 10 Variations of the lattice parameters with temperature (from room temperature to 1100 °C) in the weld pool for different filler metals: (a) γ and (b) γ'

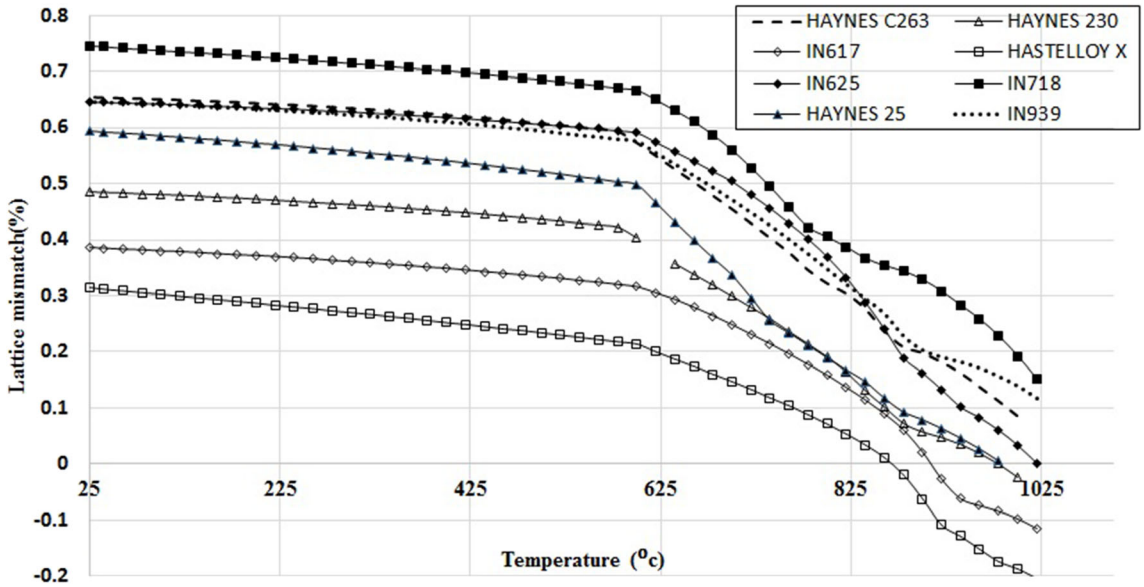

Fig. 11 Variations of the γ/γ′ lattice mismatch with temperature (from 1100 °C to ambient temperature)

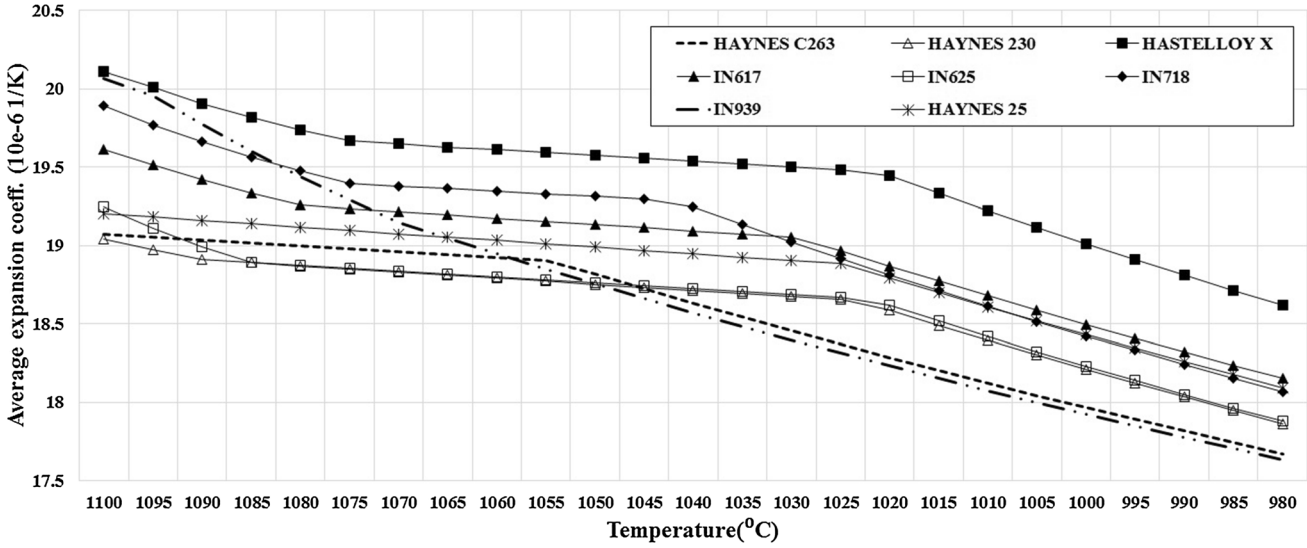

Fig. 12 Comparison of the CTE differences between the base metal and different filler metals

nickel-based superalloys increases the susceptibility to solidification cracking because of the formation of Nb-rich eutectic phases upon solidification of the weld which expands the STR. Replacing the Nb with Ta or Hf can somewhat improve these filler metals (Ref 24). Among the filler metals examined, IN625 and IN718 produced comparable results to those of other Nb-containing fillers, i.e., were more susceptible to solidification cracking than the other filler metals.

According to the results, the STRs of the weld pools produced using C263 and H230 as filler metal were generally lower than those of the other filler metals, indicating their susceptibility to solidification cracking.

4. Conclusions

The following conclusions were drawn from the present research:

1. The pre-weld heat treatment results in the complete dissolution of the secondary γ′ particles in the matrix and the growth of the primary γ′ particles in the form of "ogdoadically diced cubes" of about 2 μm in side length. Subsequently, the hardness of the base metal decreased to 310 HV.
2. The results indicated that the pre-weld heat-treated IN939 alloy is susceptible to cracking upon coarsening of the γ′

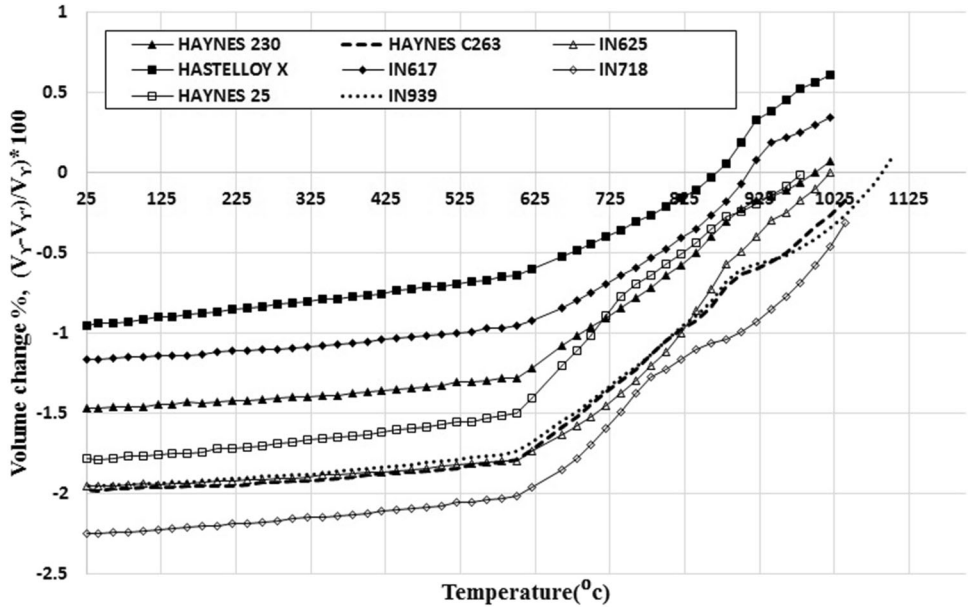

Fig. 13 Volumetric changes upon precipitation of γ′ particles in the weld pool for various filler metals

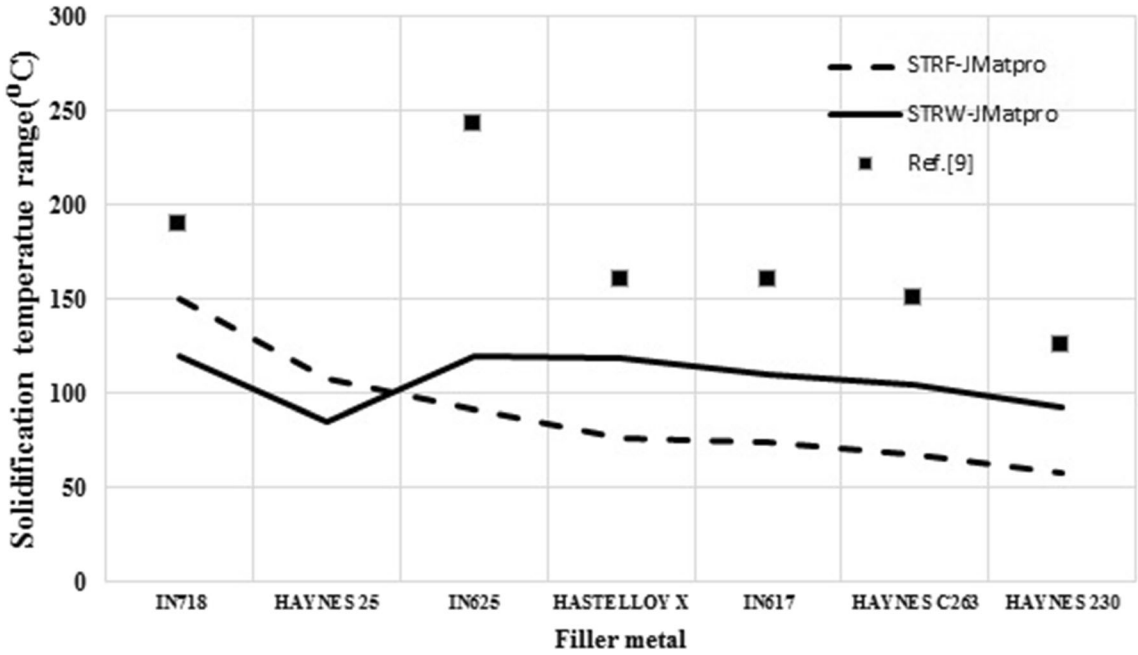

Fig. 14 Solidification temperature ranges for various filler metals

particles and the resultant partial melting. However, the strain-age cracking is much unlikely to occur during the PWHT provided the alloy is subjected to pre-weld heat treatment. The lowest amount of cracking was observed for the sample welded with HAYNES C-263 as filler metal, followed by IN617 and IN625.

3. In all of the weld pools, the observed γ′ particles were about 0.2 μm in size. The content of such particles was the highest when C623 or IN718 was used as filler metal, while HAYNES 25 and IN625 produced the lowest contents.
4. The highest hardness was measured for the sample welded with HAYNES C-263 as filler metal, implying higher strength of the welds produced by this filler metal, as compared to other filler metals studied in this study.
5. The filler metals with lower contents of (Al + Ti + Nb + Ta + Mo + W) than the base metal could effectively reduce the PWHT cracking.
6. The results indicated that among the filler metals studied in this research, HAYNES C-263, IN617 and IN625 can be considered as proper filler metals for welding IN939 alloy. However, there may be other commercially available filler metals for welding IN939 alloy which could produce even better results.

Acknowledgments

The authors would like to acknowledge help from the Niroo Research Institute (NRI) for providing the required research facilities.

Compliance with ethical standards

Conflict of interest

The authors declare that they have no conflicts of interest.

References

1. S.P. Gadewar, P. Swaminadhan, M.G. Harkare, and S.H. Gawande, Experimental Investigation of Weld Characteristics for a Single Pass TIG Welding with SS304, *Int. J. Eng. Sci. Technol.*, 2010, **2**(8), p 3676–3686
2. A. Thakur, Microstructural responses of a nickel-base cast IN-738 superalloy to a variety of pre-weld heat-treatments, Dissertation, Manitoba University, Winnipeg, 1997
3. J.C. Lippold, S.D. Kiser, and J.N. DuPont, *Welding Metallurgy and Weldability of Nickel-Base Alloys*, Wiley, Hoboken, 2011
4. T.A. Tejedor, R. Singh, and P. Pilidis, *Modern Gas Turbine Systems*, Woodhead Publishing Series in Energy, New Delhi, 2013
5. T. Gibbons and R. Stickler, *IN939: Metallurgy, properties and performance, High Temperature Alloys for Gas Turbines 1982*, Springer, London, 1982
6. C. Cutler and S. Shaw, The interrelationship of γ′ size, grain size and mechanical properties in IN-939, a cast nickel-base superalloy, the 5th International Conference, Strength of Metals and Alloys, Aachen, 1979, p 1357–1362
7. A. Athiroj, P. Wangyao, F. Hartung, and G. Lothongkum, Low heat Input Welding of Nickel Superalloy GTD-111 with Inconel 625 Filler Metal, *Mater. Test.*, 2018, **60**(1), p 22–30
8. S. Cherif and B. Zakaria, Effect of Welding Current on Microstructures and Mechanical Properties of Welded Ni-Base Superalloy INC738LC, *World J. Eng.*, 2018, **15**(1), p 14–20
9. R. Sidhu, N. Richards, and M. Chaturvedi, Effect of Aluminium Concentration in Filler Alloys on HAZ Cracking in TIG Welded Cast Inconel 738LC Superalloy, *Mater. Sci. Technol.*, 2005, **21**(10), p 1119–1131
10. K. Nishimoto, H. Mori, S. Kawaguchi, M. Toyoda, and K. Tsukimoto, Development of Filler Metal for Welding of Nickel-Base Superalloy IN738LC by Mathematical Programming Method, *Weld World*, 2002, **46**(9-10), p 19–28
11. O. Ola, O. Ojo, and M. Chaturvedi, Role of Filler Alloy Composition on Laser Arc Hybrid Weldability of Nickel-Base IN738 Superalloy, *Mater. Sci. Technol.*, 2014, **30**(12), p 1461–1469
12. K. Banerjee, N. Richards, and M. Chaturvedi, Effect of Filler Alloys on Heat-Affected Zone Cracking in Preweld Heat-Treated IN-738 LC Gas-Tungsten-Arc Welds, *Metall. Mater. Trans. A*, 2005, **36**(7), p 1881–1890
13. R. Sidhu, N. Richards, and M. Chaturvedi, Effect of Filler Alloy Composition on Post-Weld Heat Treatment Cracking in GTA Welded Cast Inconel 738LC Superalloy, *Mater. Sci. Technol.*, 2008, **24**(5), p 529–539
14. S. Kou, *Welding Metallurgy*, Wiley, Hoboken, 2003
15. A. Thakur, N. Richards, and M. Chaturvedi, On Crack-Free Welding of Cast Inconel 738, *Int. J. Join. Mater.*, 2003, **15**(5), p 21–25
16. O. Ola, O. Ojo, and M. Chaturvedi, On the Development of a New Pre-weld Thermal Treatment Procedure for Preventing Heat-Affected Zone (HAZ) Liquation Cracking in Nickel-Base IN 738 Superalloy, *Philos. Mag.*, 2014, **94**(29), p 3295–3316
17. R. Ricks, A. Porter, and R. Ecob, The Growth of γ′ Precipitates in Nickel-Base Superalloys, *Acta Metall.*, 1983, **31**(1), p 43–53
18. M. Doi, T. Miyazaki, and T. Wakatsuki, The Effect of Elastic Interaction Energy on the Morphology of γ′ Precipitates in Nickel-Based Alloys, *Mater. Sci. Eng.*, 1984, **67**(2), p 247–253
19. H.B. Aaron and G.R. Kotler, Second Phase Dissolution, *Metall. Trans.*, 1971, **2**(2), p 393–408
20. K.C. Chen, T.C. Chen, R.K. Shiue, and L.W. Tsay, Liquation Cracking in the Heat-Affected Zone of IN738 Superalloy Weld, *Metals*, 2018, **8**(6), p 387
21. M. Nathal, R. Mackay, and R. Garlick, Temperature Dependence of γ-γ′ Lattice Mismatch in Nickel-Base Superalloys, *Mater. Sci. Eng.*, 1985, **75**(1-2), p 195–205
22. M.A. Gonzalez Albarran, D. Martinez, E. Diaz, J.C. Diaz, I. Guzman, E. Saucedo, and AMa Guzman, Effect of preweld heat treatment on the microstructure of heat-affected zone (HAZ) and weldability of Inconel 939 superalloy, *J. Mater. Eng. Perform.*, 2014, **23**(4), p 1125–1130
23. J.C. Lippold, J.W. Sowards, G.M. Murray, B.T. Alexandrov, and A.J. Ramirez, Weld Solidification Cracking in Solid-Solution Strengthened Ni-Base Filler Metals, in *Hot Cracking Phenomena in Welds II*., 2008, Springer, p 147–170
24. A.T. Hope and J.C. Lippold, Development and Testing of a High-Chromium, Ni-Based Filler Metal Resistant to Ductility Dip Cracking and Solidification Cracking, *Weld Word*, 2017, **61**(2), p 325–332